Check for updates

Assessing the impact of posture on brain volume in healthy subjects with a rotatable cryogen-free 1.5T superconducting MRI

Shiying Ke[1,2], Yulin Wang[1], Jichang Zhang[1,3], Jie Zeng[1],
Shengyang Niu[1], Jianjun Zheng[4], Thomas Meersmann[5,6,7] and
Chengbo Wang[1]*

[1]Department of Electrical and Electronic Engineering, Faculty of Science and Engineering, University
of Nottingham Ningbo China, Ningbo, China, [2]Department of Medical Imaging, Quanzhou Medical
College, Quanzhou, China, [3]Xingaoyi Medical Equipment Company, Ltd., Ningbo, China, [4]Department
of Radiology, Ningbo No. 2 Hospital, Ningbo, China, [5]School of Medicine, Sir Peter Mansfield Imaging
Centre, Translational Medical Sciences, University of Nottingham, Nottingham, United Kingdom,
[6]NIHR Nottingham Biomedical Research Centre, Nottingham University Hospitals NHS Trust, Queen's
Medical Centre, Nottingham, United Kingdom, [7]Department for Strategic Development of Health
Science and Technology, University of Nottingham Ningbo China, Ningbo, Zhejiang, China

Background: Magnetic Resonance Imaging (MRI) is crucial for detailed
visualization of brain structure and function. However, conventional supine
imaging limits the exploration of how posture impacts brain morphology. While
recent advancements in upright MRI systems have enabled studies of postural
effects on various body systems, investigations into posture's impact on brain
anatomy remain limited.

Method: This study investigated volumetric differences between upright and
supine positions to establish a baseline for future investigations into how
posture influenced brain structure. Thirty-one healthy volunteers underwent
scans using a rotatable cryogen-free 1.5T MRI scanner in supine and upright
postures. The 3D T1-weighted MP-RAGE brain images were segmented into 109
regions, and volume changes across these regions were analyzed.

Result: Volumetric analysis across 109 brain regions in both supine and upright
postures shows minimal changes, with most regions displaying variations within
a $\pm 5\%$ range. The coefficient of variation (COV) indicated that posture-induced
volume changes are even smaller than the measurement precision of the
method. These findings provide a solid groundwork for future studies on the
effects of posture on brain structure.

Conclusion: The majority of brain regions exhibited no significant volumetric
differences between supine and upright positions, suggesting that brain
structure remains consistent and stable across different postures. These findings
offer valuable insights for future research on the postural influences on brain
morphology.

KEYWORDS

MRI, brain structures, volumetric differences, postural effects, MP-RAGE

1 Introduction

Magnetic Resonance Imaging (MRI) has emerged as a crucial tool for visualizing brain structures and functions due to its non-invasive nature, high spatial resolution, and ability to provide detailed anatomical and functional insights (Thompson et al., 2005).

Traditionally, most MRI scans are conducted with subjects in a supine position, a practice necessitated by the design constraints of conventional MRI scanners (Eşer et al., 2007). Although effective for many diagnostic purposes, this fixed, non-physiological posture may not fully represent how brain structures and functions operate, as human bodies are typically more dynamic and engage in various postures in daily life (Alperin et al., 2005a). Posture is known to significantly influence physiological and anatomical characteristics across the body. For example, shifting from lying down standing can alter spinal alignment, change lung capacity, and modify cardiovascular dynamics, among other effects (Rossberg and Peňaz, 1988; Fawcett et al., 2021). These observations underscore the importance of incorporating different postures in studies of body systems and their functions. However, traditional MRI systems are limited in their ability to assess posture-related structural differences, highlighting the need for innovative multi-positional MRI technologies.

To overcome these limitations, researchers have introduced various MRI systems capable for upright or weight-bearing imaging, including Fonar's 0.6T system (Nicholson et al., 2023), Siemens' 1.0T system (Gufler et al., 2004), and G-Scan's 0.25T system (Lee et al., 2015b), et al. Although these systems operate at relatively low magnetic field strengths, which may reduce image resolution and signal-to-noise ratio (SNR) during scanning (Marques et al., 2019), they have proven the research value in the effects of specific postures on body structures (Shymon et al., 2014; Hansen et al., 2019). The 1.5T MRI system provides higher SNR and spatial resolution, allowing for clearer visualization of small lesions and anatomical structures, thus enhancing the quantitative analysis capabilities of the images and assisting clinicians in making more accurate diagnostic and treatment decisions (Magee et al., 2003; Arnold et al., 2023; Schmid et al., 1999). For instance, upright MRI has proven notably effective in detecting spinal stenosis (Fawcett et al., 2021) and in visualizing medial meniscus extrusion in the knee under weight-bearing conditions (Draper et al., 2011). Additionally, these systems offer significant benefits in the early diagnosis of pelvic organ prolapse (Shaikh et al., 2021), thereby facilitating more prompt and effective treatment. Despite significant technological advancements, most existing studies have focused on other body systems, leaving research on the impact of posture on brain morphology relatively underexplored. Regions of the brain, such as the pituitary gland, cerebellum, and choroid plexus, which are more susceptible to gravitational effects, are particularly affected. A previous study has shown that the choroid plexus undergoes morphological changes under the influence of gravity (Wang et al., 2025). These findings highlight the gap in our understanding of how posture affects brain structure and emphasize the pressing need for innovative MRI systems specifically designed for brain research.

While traditional MRI systems and some newly developed upright MRI systems have significantly advanced our understanding of postural effects on other body systems, research in the brain domain remains limited due to technical and methodological challenges. In prior studies, the evaluation of brain regions in the upright posture was typically done through visual assessment by two blinded clinicians, without image segmentation. This approach likely arose from the lack of automatic segmentation technology available in 2001, and the image quality at that time may not have met the requirements for accurate segmentation (Nakada and Tasaka, 2001). Additionally, there was relatively limited research on upright head imaging. To address these challenges, we have developed a cryogen-free 1.5T superconductive MRI system that can operate with an active magnetic field during scanner rotation (Wang et al., 2023). This system offers a unique opportunity to study the impact of different postures on brain morphology under conditions that closely mimic everyday physiological activities. This innovative design allows for high-resolution imaging in both supine and upright positions without compromising image quality.

The objective of this study is to investigate and validate whether significant volumetric changes occur in various brain regions between upright and supine positions in healthy individuals. By identifying and quantifying these differences, we aim to elucidate the potential clinical implications of postural effects on brain structure. These findings could offer valuable insights for advancing clinical brain research, especially in conditions where postural influences may play a significant role.

2 Method

All imaging was conducted using a state-of-the-art, rotatable, cryogen-free superconductive 1.5T MRI scanner (XGY-Spin MRI-R001, XGY, Ningbo, China), which served as the primary imaging platform (Figure 1). This prospective study was carried out between August to September 2024, with ethical approval granted by the institutional ethics committees of both the University of Nottingham Ningbo China, and Ningbo No. 2 Hospital. Written informed consent was obtained from all participants, ensuring compliance with established guidelines for human research. Additionally, participant confidentiality was meticulously maintained by anonymizing data prior to analysis.

The inclusion criteria for eligible participants were aged 20–35 years, without any history of neurological or psychiatric disorders, and met all MRI scanning safety requirements. The exclusion criteria included significant brain abnormalities, a history of brain surgery, systemic diseases affecting brain structure (e.g., hypertension or diabetes), or pregnancy. Initially, 33 individuals were enrolled; however, one was excluded due to the presence of a cerebral lipoma. Additionally, due to a computer system error, data from one individual was corrupted, leading to exclusion. As a result, the final cohort consisted of 31 healthy volunteers (mean age: 26.5 ± 3.7 years; comprising 16 males and 15 females). Each subject underwent an MRI scan using a 3D T1-weighted MPRAGE sequence, with the following settings: Repetition Time (TR) = 10.0 ms, Echo Time (TE) = 3.4 ms, Field of View (FOV) = 230 mm × 230 mm × 187.2 mm, Sampling Matrix = 192 × 192 × 156, Reconstruction Matrix = 480 × 480 × 156, Spatial Resolution = 0.48 mm × 0.48 mm × 1.20 mm, Slice Thickness = 1.20 mm, and Flip Angle = 12°. The scan time for the 3D MP-RAGE sequence was 4 min and 15 s. Scans were performed in two different postures—supine (0 degrees) and upright (90 degrees). For supine scans, participants' heads were supported by foam pads to minimize motion. In the upright posture, restraint straps and

FIGURE 1
Design and configuration of the 1.5T superconductive cryogen-free spin MRI system: **(a)** at 0° angle for supine scanning, **(b)** at 45° angle for an oblique view, and **(c)** at 90° angle for upright scanning.

additional foam pads were used to secure and align the head, effectively reducing motion artifacts.

A comprehensive volumetric analysis of 109 brain regions was performed using the United Imaging analysis system to assess structural changes between the two postures. The automated whole-brain segmentation from 3D T1-weighted MPRAGE images was conducted via the uAI Research Portal (United Imaging Intelligence, China) (Wu et al., 2023), a clinical research platform developed using Python (version 3.7.3). This process utilized the PyRadiomics package[1] (Liu et al., 2022), enabling precise segmentation of the whole brain into 109 distinct regions and providing volumetric measurements for each region to assess structural changes between the two postures (Figure 2).

To assess both the reproducibility and repeatability of this analysis method, an experiment was conducted with three selected subjects. Measurements of brain volume in the supine posture were performed for each subject at three time points: Day 1 (first scan), Day 30 (second scan, initial scan), and Day 30 (third scan, taken 30 min after the second scan). This approach aimed to determine the stability of measurements over time and the reliability of the method. The coefficient of variation (COV) (Bland and Altman, 2010) was calculated using the formula: COV = (Standard deviation/Mean) × 100% (Abdi, 2010). And the average COV was calculated across the three subjects. In this study, the COV was expressed as a percentage, providing a depiction of measurement variability and aiding in the assessment of the precision and consistency of the measurements.

Subsequently, brain volume was measured in both the supine and upright positions for all 31 subjects to evaluate changes in brain region volumes between these two postures. Additionally, the percentage change in brain volume between the upright and supine measurements was calculated using the formula: $(V_{upright} - V_{supine})/(V_{upright}) \times 100\%$, where V_{supine} and $V_{upright}$ represent the brain volume in the supine and upright postures, respectively. To ensure the validity of the parametric analysis, the Shapiro–Wilk test was conducted for each brain region to assess whether the volume data conformed to a normal distribution. Only regions that satisfied the normality assumption were included in the subsequent two-tailed paired Student's t-test. For regions that did not meet the normality assumption, the non-parametric Wilcoxon signed-rank test was applied instead. These statistical tests were used to evaluate volume differences between the two positions. Multiple comparison corrections were also applied to control for Type 1 errors.

3 Results

Table 1 presents the demographic characteristics of the participants, all of whom are young adults. This selection minimizes the influence of age-related brain volume decline. Additionally, the balanced gender ratio helps reduce the potential impact of sex differences on brain structure.

Imaging was conducted on all subjects using the spin MRI, with no adverse effects. Figure 2 illustrates the segmentation of 109 distinct brain regions from 3D T1-weighted MPRAGE images of a sample subject in both upright and supine positions, performed using the uAI Research Portal. Volumetric measurements for each region were obtained to evaluate structural differences between the two positions.

As shown in Figure 3, the average COV across the three subjects was 4.61% ± 2.60%, indicating good measurement repeatability. The COV values remained consistent across the three time points: Day 1 (first scan), Day 30 (second scan, initial scan), and Day 30 (third scan, conducted 30 min after the second scan). The absence of significant fluctuation further suggests that the scanning method provides reliable precision and temporal stability. Overall, the low mean COV reflects the high repeatability and low variability of the brain volume measurements in the supine posture.

To further assess the measurement precision of the scanning method, we calculated the coefficient of variation (COV) for brain volume measurements in three subjects across the three designated time points: Day 1 (first scan), Day 30 (second scan, initial scan), and Day 30 (third scan, conducted 30 min after the second scan). For each subject, the COV was determined by dividing the standard deviation of the three volume measurements by their mean (Figure 3b). The final mean COV was obtained by averaging the individual COV values across the three subjects (Figure 3a).
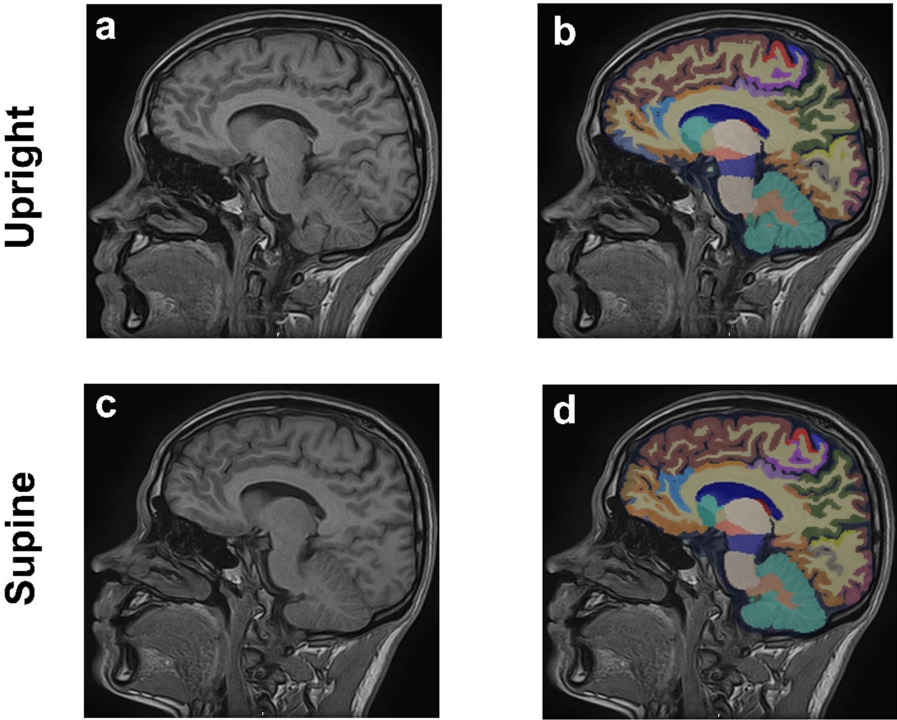
---

1 https://pyradiomics.readthedocs.io

FIGURE 2
Sagittal 3D T1-weighted MPRAGE MRI images of the brain from a 29-year-old male in upright **(a,b)** and supine **(c,d)** positions. Anatomical images are shown in **(a,c)**, **(b,d)** corresponding regional brain segmentations.

TABLE 1 Demographic characteristics of the study participants.

Normal volunteers	Pre-scan	Post-scan	p value
Age (years)	26.5 ± 3.7		
Gender (M/F)	16/15		
Height (cm)	168.8 ± 6.6		
Weight (kg)	64.8 ± 11.7		
HR (beats/min)	78.9 ± 13.8	76.7 ± 11.6	0.501
Systolic BP (mmHg)	115.2 ± 12.6	110.5 ± 11.7	0.148
Diastolic BP (mmHg)	74.1 ± 7.2	70.9 ± 7.5	0.101

HR, heart rate; BP, blood pressure.

Figure 4 shows the overlap of the coefficient of variation (COV) values with the percentage volume changes across 109 brain regions between upright and supine postures. The gray bars represent brain regions with volume changes within the ±5% range, while the blue bars indicate regions with volume changes exceeding 5%. Most brain regions exhibit volume changes within the ±5% range, with only a few regions exceeding this threshold, suggesting that the volume changes between the two postures are very stable for the majority of brain regions.

Figure 4 illustrates that most of the gray bars, representing the average postural volume changes across the 31 subjects, fall within the red box, which denotes the average COV across the three selected subjects for each segmented brain region. This suggests that most brain regions are highly stable, with their postural changes resembling those observed in the same supine posture across different time points.

Figure 5 presents a scatter plot illustrating the relationship between percentage volume changes and p-values. The majority of brain regions display minimal volume changes, with p-values approaching 1, whereas a few regions near the threshold of significance with p-values close to 0.05, further underscoring the overall stability of brain volumes. Multiple comparison corrections were also applied, and the results remained consistent, reinforcing the stability and robustness of the observed findings.

Most brain regions exhibited minimal volume changes between upright and supine postures. Notably, there was no significant difference in intracranial volume (ICV) between the two positions: supine position ICV was 1407981.60 ± 138923.61 mm^3, and upright position ICV was 1402848.68 ± 135176.12 mm^3 ($p = 0.89$). Figure 6a demonstrates that the Inferior Lateral Ventricle showed the most substantial negative volume change (-18.56%), which exceeded the ±5% threshold; however, this difference was not statistically significant ($p = 0.27$). In contrast, the hippocampus depicted in Figure 6b showed a negligible volume change of 0.01% ($p = 0.97$), exemplifying the typical stability observed across most brain regions. Figure 6c highlights the Choroid Plexus, which showed the largest positive volume change at 3.19% ($p = 0.64$), yet maintained a relatively stable distribution.

4 Discussion

To the best of our knowledge, this study is the first to employ a cryogen-free, rotatable superconductive MRI system in the
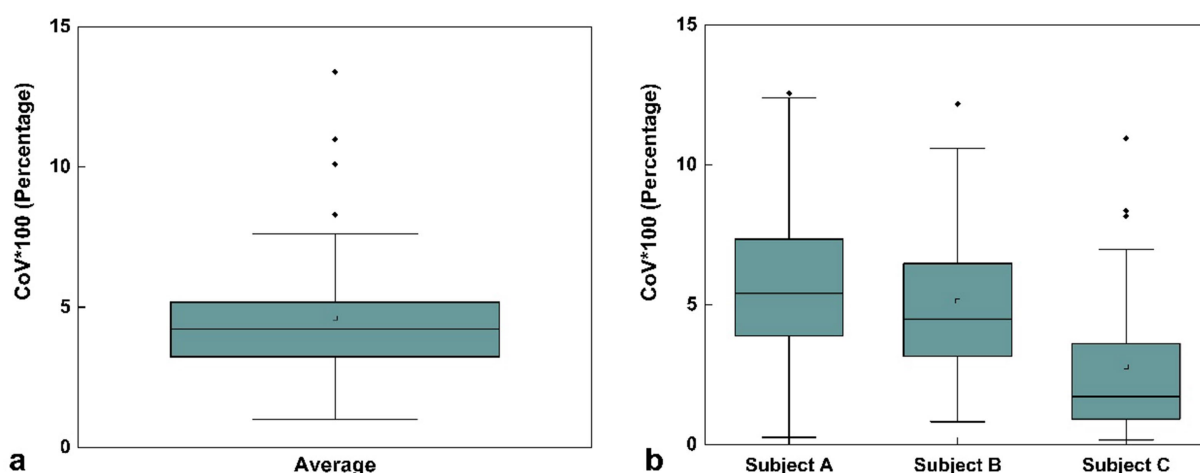
FIGURE 3
Box plot of mean coefficient of variation (COV) values for volume measurements across three time points: first scan on Day 1, second scan on Day 30 (initial scan), and third scan on Day 30 (30 min after the second scan) for three selected subjects in the same supine posture. **(a)** COV values averaged across all three subjects. **(b)** COV values for each individual subject (Subject A, Subject B, and Subject C) with three repeated scans. The square markers represent the mean values. Data represent the COV values across all 109 brain regions.

investigation of brain volume changes. While the system is capable of maintaining a continuous magnetic field during scanner rotation, it is important to note that all scans in this study were conducted at fixed positions (either 0 or 90 degrees), rather than during continuous rotation. We investigated the effects of postural changes on brain volume in healthy individuals by comparing supine and upright positions using this innovative rotatable MRI scanner, quantifying the statistical differences between these two postures. Our results indicate that postural changes have a minimal impact on brain volume in healthy individuals, which supports existing knowledge about the high stability of brain structure.

Specifically, the volume changes in most brain regions between the upright and supine positions were within a ±5% range, with the majority of regions showing near-zero volume changes and *p*-values close to 1, further validity the stability and reliability of the brain structure. This is consistent with prior upright MRI studies, which have shown that gravity exerts a negligible effect on brain structure, even in conditions such as brain atrophy (Nakada and Tasaka, 2001). However, as illustrated in Figure 6a, the inferior lateral ventricle, where CSF is contained and circulated through, showed a positive shift in volume from upright to supine, yet the overall variability remained low. This region, adjacent to cerebrospinal fluid (CSF)-filled areas, has been documented in prior research to experience a significant increase in CSF flow when supine, suggesting that these regions may be more susceptible to postural changes and may exhibit unique anatomical or hemodynamic characteristics (Muccio et al., 2021; Alperin et al., 2015). Previous studies have reported that CSF flow, velocity, and stroke volume decrease significantly in the upright posture, with these changes closely related to body position (Yukun et al., 2025). Although our study did not include direct CSF flow measurements, the volumetric trend observed may reflect posture-dependent redistribution of CSF. These findings provide preliminary structural evidence that may contribute to understanding how posture influences CSF dynamics.

Further investigations integrating structural, functional, and flow-sensitive imaging modalities are warranted to elucidate the mechanisms by which posture influences CSF distribution and ventricular morphology.

Furthermore, previous studies have demonstrated that, compared to the supine position, the upright posture reduces CSF oscillatory volume by approximately 48%, significantly increases intracranial compliance (ICC), and decreases intracranial pressure (ICP) by approximately 2.4 times (Alperin et al., 2005b). These findings highlights the dynamic role of CSF in regulating intracranial pressure across different postural orientations, effectively maintaining intracranial pressure equilibrium. Notably, prior research has also shown that, even in cases of cerebrospinal fluid leakage, brain imaging differences between the upright and supine positions remain insignificant (Schievink and Tourje, 2007). This further underscores that, despite the significant effects of upright posture on CSF distribution and ICP, the brain's intrinsic regulatory mechanisms ensure the stability of volume and morphology across brain regions (Lee et al., 2015a).

On the other hand, the hippocampus (Figure 6b) demonstrated the overall stability of most brain regions, with minimal variation between postures. Likewise, despite relatively larger volume changes in the choroid plexus, its low variability further highlights the consistency of measurements across different postural conditions.

The results depicted in Figure 3 demonstrate the good precision and repeatability of the current method. Measurement values for all three subjects exhibited minimal fluctuation across different time points indicating that the method provides consistent volume measurements. By calculating COV, we found that the measurement consistency for the vast majority of brain regions is high, indicating that the current measurement method demonstrates good repeatability and stability. The volume changes in brain regions induced by posture shifts mostly fall within the measurement error range, making them undetectable by the current method.
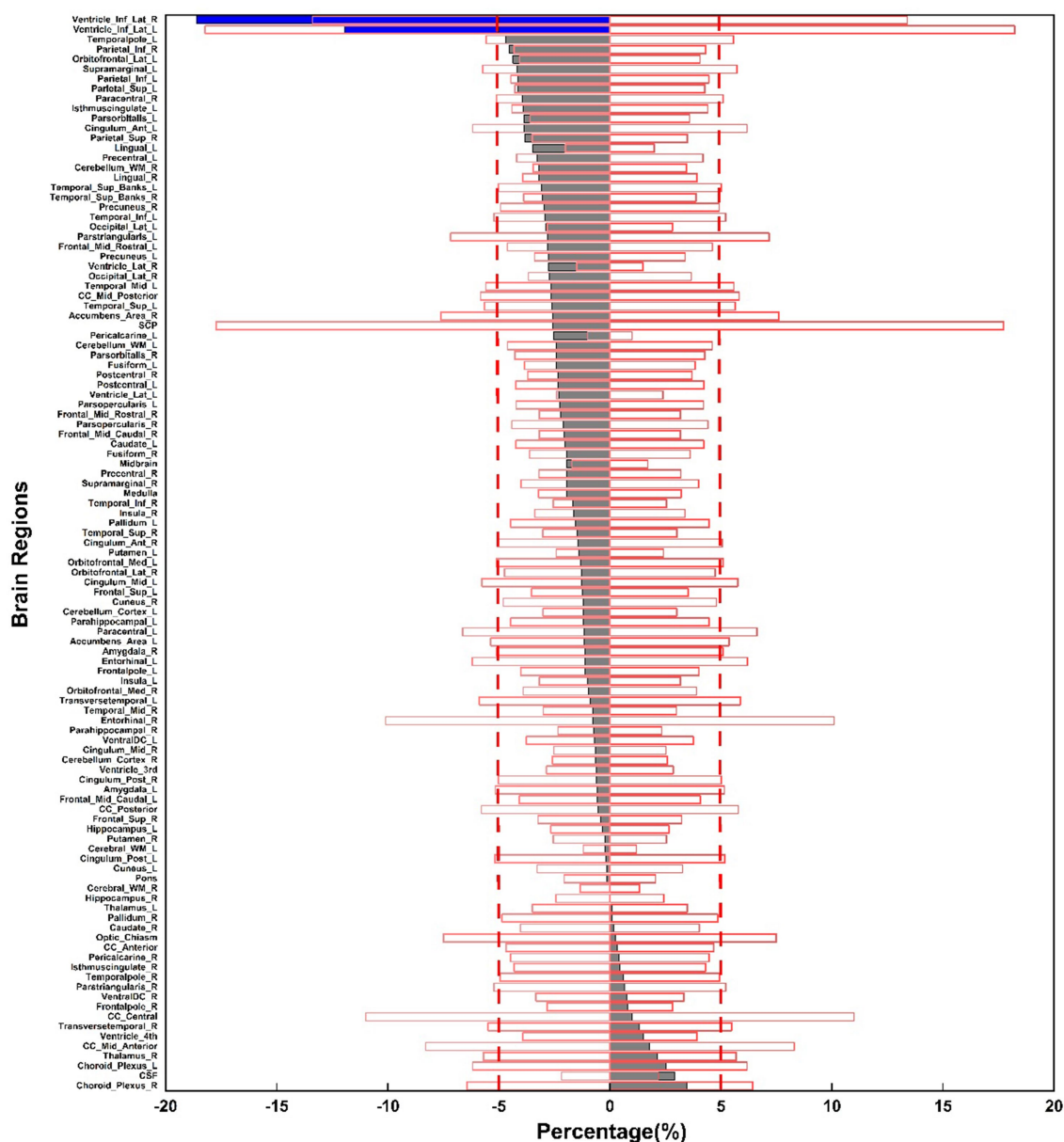
FIGURE 4
Percentage volume changes between upright and supine postures across 109 brain regions, illustrated in the gray and blue bars. The red box displays the mean COV values for volume measurements across three selected subjects at three time points.

5 Limitation

A limitation of this study is that the COV measurements were derived from data obtained from only three subjects. Such a small sample size may not be sufficiently robust to provide a comprehensive evaluation of the precision and consistency of the method at this scale. Although the results indicate that the method operates effectively within a reasonable margin, the limited sample size could introduce variability in the accuracy of the measurements. To achieve a more reliable estimation of the COV, it would be ideal to conduct multiple scans with a larger cohort, each undergoing at least three separate measurements. However, implementing such a protocol would significantly extend the required scanning time and necessitate

multiple visits from the volunteers, which presents considerable logistical challenges. Consequently, the COV values observed in this study may not fully reflect the true precision of the method, highlighting the need for further studies involving larger sample sizes and repeated scans to confirm the reliability and generalizability of the findings.

Another limitation of this study concerns the accuracy of choroid plexus segmentation. Although we utilized the PyRadiomics package for segmentation of 109 brain regions, the tool is based on FreeSurfer, which has shown limited performance in choroid plexus segmentation (Zhao et al., 2020). As the choroid plexus is a critical structure influenced by body position and CSF flow, previous studies have demonstrated that deep learning-based approaches

perform significantly better in this context (Yazdan-Panah et al., 2023; Eisma et al., 2024; Zhao et al., 2020). However, due to the scope of this study, these advanced deep learning techniques were not implemented. It is worth noting that a parallel study using this rotatable MRI system has analyzed the choroid plexus and provides supplementary data (Wang et al., 2025). We acknowledge that the segmentation method used in this study may not provide the same level of precision as newer techniques, which may affect the reliability of the volumetric findings related to the choroid plexus. In future work, we plan to explore these advanced deep learning techniques to improve segmentation accuracy.

6 Conclusion

In conclusion, while most brain regions showed no significant differences between supine and upright positions, these findings

FIGURE 5
Scatter plot of percentage volume change versus *p*-values for 109 segmented brain regions. The x-axis represents the percentage change, while the y-axis shows p-values. Red dashed lines mark ±5% on the x-axis and a significance level of 0.05 on the y-axis, where each triangle represents a brain region.

deepen our understanding of the potential clinical implications of postural effects on brain structure and provide valuable insights for future studies in clinical brain research.
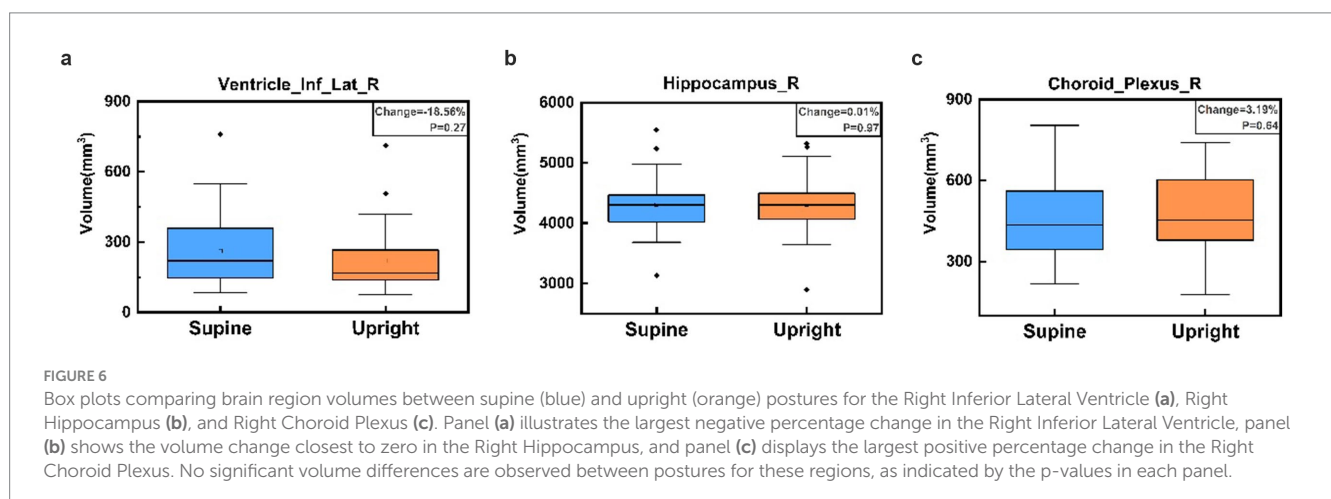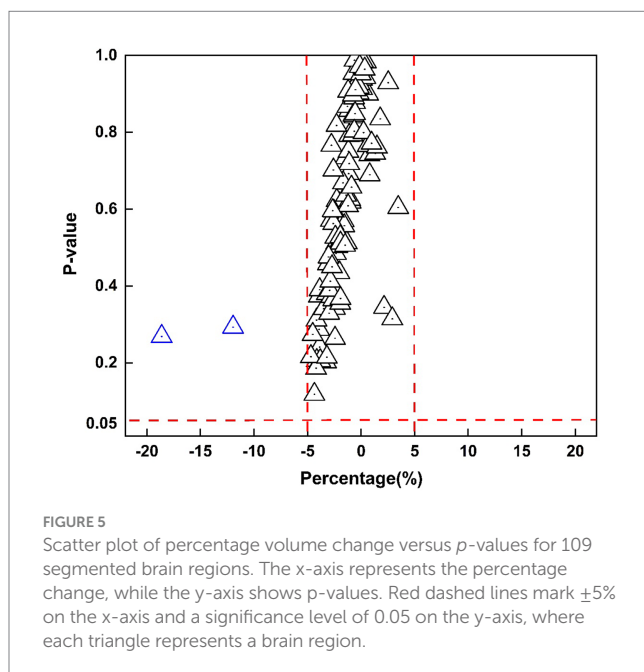
Author's note

Parts of this work have been presented as a digital poster at the 33rd Annual Meeting of the International Society for Magnetic Resonance in Medicine (ISMRM), 2025.

Data availability statement

The datasets presented in this article are not readily available because this prospective study was approved by the institutional ethics committees of both the University of Nottingham Ningbo China and Ningbo No. 2 Hospital. Participant confidentiality was carefully maintained by anonymizing the data prior to analysis. Due to sensitivity concerns, the data supporting the findings of this study are not openly available. Access to the data may require institutional or ethical approval due to privacy considerations. Further, the data are available from the corresponding author upon reasonable request. Requests to access the datasets should be directed to chengbo.wang@nottingham.edu.cn.

Ethics statement

The studies involving humans were approved by ethical approval granted by the institutional ethics committees of both the University of Nottingham Ningbo China, and Ningbo No. 2 Hospital. Written informed consent was obtained from all participants, ensuring compliance with established guidelines for human research. The studies were conducted in accordance with the local legislation and institutional requirements. The participants provided their written informed consent to participate in this study. Written informed consent was obtained from the individual(s) for the publication of any potentially identifiable images or data included in this article.

FIGURE 6
Box plots comparing brain region volumes between supine (blue) and upright (orange) postures for the Right Inferior Lateral Ventricle (a), Right Hippocampus (b), and Right Choroid Plexus (c). Panel (a) illustrates the largest negative percentage change in the Right Inferior Lateral Ventricle, panel (b) shows the volume change closest to zero in the Right Hippocampus, and panel (c) displays the largest positive percentage change in the Right Choroid Plexus. No significant volume differences are observed between postures for these regions, as indicated by the p-values in each panel.

Author contributions

SK: Conceptualization, Data curation, Formal analysis, Methodology, Resources, Software, Validation, Visualization, Writing – original draft, Writing – review & editing. YW: Data curation, Methodology, Software, Validation, Writing – review & editing. JicZ: Data curation, Methodology, Validation, Writing – review & editing. JieZ: Data curation, Writing – review & editing. SN: Data curation, Writing – review & editing. JiaZ: Investigation, Resources, Writing – review & editing. TM: Methodology, Project administration, Writing – review & editing. CW: Methodology, Project administration, Writing – review & editing.

Funding

Conflict of interest

JZ was employed by Xingaoyi Medical Equipment Company, Ltd.

The remaining authors declare that the research was conducted in the absence of any commercial or financial relationships that could be construed as a potential conflict of interest.

Generative AI statement

The authors declare that no Gen AI was used in the creation of this manuscript.

Any alternative text (alt text) provided alongside figures in this article has been generated by Frontiers with the support of artificial intelligence and reasonable efforts have been made to ensure accuracy, including review by the authors wherever possible. If you identify any issues, please contact us.

Publisher's note

References

Abdi, H. (2010). "Coefficient of variation" in Encyclopedia of research design, 2010•utdallas.edu, vol. 1, 169–171.

Alperin, N., Hushek, S., Lee, S., Sivaramakrishnan, A., and Lichtor, T. (2005a). Mri study of cerebral blood flow and CSF flow dynamics in an upright posture: The effect of posture on the intracranial compliance and pressure. Intracranial pressure and brain monitoring XII. Acta Neurochirurgica-supplementum then supplement-Wien: Springer, 177–181.

Alperin, N., Lee, S. H., and Bagci, A. M. (2015). MRI measurements of intracranial pressure in the upright posture: the effect of the hydrostatic pressure gradient. *J. Magn. Reson. Imaging* 42, 1158–1163. doi: 10.1002/jmri.24882

Alperin, N., Lee, S. H., Sivaramakrishnan, A., and Hushek, S. G. (2005b). Quantifying the effect of posture on intracranial physiology in humans by MRI flow studies. *J. Magn. Reson. Imaging* 22, 591–596. doi: 10.1002/jmri.20427

Arnold, T. C., Freeman, C. W., Litt, B., and Stein, J. M. (2023). Low-field MRI: clinical promise and challenges. *J. Magn. Reson. Imaging* 57, 25–44. doi: 10.1002/jmri.28408

Bland, J. M., and Altman, D. G. (2010). Statistical methods for assessing agreement between two methods of clinical measurement. *Int. J. Nurs. Stud.* 47, 931–936. doi: 10.1016/j.ijnurstu.2009.10.001

Draper, C. E., Besier, T. F., Fredericson, M., Santos, J. M., Beaupre, G. S., Delp, S. L., et al. (2011). Differences in patellofemoral kinematics between weight-bearing and non-weight-bearing conditions in patients with patellofemoral pain. *J. Orthop. Res.* 29, 312–317. doi: 10.1002/jor.21253

Eisma, J. J., Mcknight, C. D., Hett, K., Elenberger, J., Han, C. J., Song, A. K., et al. (2024). Deep learning segmentation of the choroid plexus from structural magnetic resonance imaging (MRI): validation and normative ranges across the adult lifespan. *Fluids Barriers CNS* 21:21. doi: 10.1186/s12987-024-00525-9

Eşer, İ., Khorshid, L., Yapucu Güneş, Ü., and Demir, Y. (2007). The effect of different body positions on blood pressure. *J. Clin. Nurs.* 16, 137–140. doi: 10.1111/j.1365-2702.2005.01494.x

Fawcett, L., James, S., Botchu, R., Martin, J., Heneghan, N. R., and Rushton, A. (2021). The influence of spinal position on imaging findings: an observational study of thoracolumbar spine upright MRI in elite gymnasts. *Eur. Spine J.* 31, 1–8. doi: 10.1007/s00586-021-06997-9

Gufler, H., Ohde, A., Grau, G., and Grossmann, A. (2004). Colpocystoproctography in the upright and supine positions correlated with dynamic MRI of the pelvic floor. *Eur. J. Radiol.* 51, 41–47. doi: 10.1016/S0720-048X(03)00133-5

Hansen, B. B., Nordberg, C. L., Hansen, P., Bliddal, H., Griffith, J. F., Fournier, G., et al. (2019). Weight-bearing MRI of the lumbar spine: spinal stenosis and spondylolisthesis. *Semin. Musculoskelet. Radiol.* 23, 621–633. doi: 10.1055/s-0039-1697937

Lee, R. K., Griffith, J. F., Leung, J. H., Chu, W. C., Lam, T., Ng, B. K., et al. (2015b). Effect of upright position on tonsillar level in adolescent idiopathic scoliosis. *Eur. Radiol.* 25, 2397–2402. doi: 10.1007/s00330-015-3597-3

Lee, H., Xie, L., Yu, M., Kang, H., Feng, T., Deane, R., et al. (2015a). The effect of body posture on brain glymphatic transport. *J. Neurosci.* 35, 11034–11044. doi: 10.1523/JNEUROSCI.1625-15.2015

Liu, S., Jie, C., Zheng, W., Cui, J., and Wang, Z. (2022). Investigation of underlying association between whole brain regions and Alzheimer's disease: a research based on an artificial intelligence model. *Front. Aging Neurosci.* 14:872530. doi: 10.3389/fnagi.2022.872530

Magee, T., Shapiro, M., and Williams, D. (2003). Comparison of high-field-strength versus low-field-strength MRI of the shoulder. *Am. J. Roentgenol.* 181, 1211–1215. doi: 10.2214/ajr.181.5.1811211

Marques, J. P., Simonis, F. F., and Webb, A. G. (2019). Low-field MRI: an MR physics perspective. *J. Magn. Reson. Imaging* 49, 1528–1542. doi: 10.1002/jmri.26637

Muccio, M., Chu, D., Minkoff, L., Kulkarni, N., Damadian, B., Damadian, R. V., et al. (2021). Upright versus supine MRI: effects of body position on craniocervical CSF flow. *Fluids Barriers CNS* 18:61. doi: 10.1186/s12987-021-00296-7

Nakada, T., and Tasaka, N. (2001). Human brain imaging in the upright position. *Neurology* 57, 1720–1722. doi: 10.1212/WNL.57.9.1720

Nicholson, L. L., Rao, P. J., Lee, M., Wong, T. M., Cheng, R. H. Y., and Chan, C. (2023). Reference values of four measures of craniocervical stability using upright dynamic magnetic resonance imaging. *Radiol. Med.* 128, 330–339. doi: 10.1007/s11547-023-01588-8

Rossberg, F., and Peňaz, J. (1988). Initial cardiovascular response on change of posture from squatting to standing. *Eur. J. Appl. Physiol. Occup. Physiol.* 57, 93–97. doi: 10.1007/BF00691245

Schievink, W. I., and Tourje, J. (2007). Upright MRI in spontaneous spinal cerebrospinal fluid leaks and intracranial hypotension. *Headache* 47, 1345–1346. doi: 10.1111/j.1526-4610.2007.00934.x

Schmid, M. R., Stucki, G., Duewell, S., Wildermuth, S., Romanowski, B., and Hodler, J. (1999). Changes in cross-sectional measurements of the spinal canal and intervertebral foramina as a function of body position: in vivo studies on an open-configuration MR system. *AJR Am. J. Roentgenol.* 172, 1095–1102. doi: 10.2214/ajr.172.4.10587155

Shaikh, N., Zhang, H., Brown, S. H., Lari, H., Lasry, O., Street, J., et al. (2021). Synchronous imaging of pelvic geometry and muscle morphometry: a pilot study of pelvic retroversion using upright MRI. *Sci. Rep.* 11:20127. doi: 10.1038/s41598-021-99305-w

Shymon, S., Hargens, A. R., Minkoff, L. A., and Chang, D. G. (2014). Body posture and backpack loading: an upright magnetic resonance imaging study of the adult lumbar spine. *Eur. Spine J.* 23, 1407–1413. doi: 10.1007/s00586-014-3247-5

Thompson, P. M., Sowell, E. R., Gogtay, N., Giedd, J. N., Vidal, C. N., Hayashi, K. M., et al. (2005). Structural MRI and brain development. *Int. Rev. Neurobiol.* 67, 285–323. doi: 10.1016/S0074-7742(05)67009-2

Wang, Y., Ke, S., Li, J., Zeng, J., Zhang, J., Niu, S., et al. (2025). Assessing morphological changes in the choroid plexus between standing and supine positions using a rotatable MRI system. *Sci. Rep.* 15:22329. doi: 10.1038/s41598-025-07985-5

Wang, Y., Wang, S., Liang, P., Brusic, V., Zeng, J., Liu, B., et al. (2023). Design, construction and performance testing of a 1.5 T cryogen-free low-temperature superconductor whole-body MRI magnet. *Supercond. Sci. Technol.* 36:045002. doi: 10.1088/1361-6668/acb467

Wu, J., Xia, Y., Wang, X., Wei, Y., Liu, A., Innanje, A., et al. (2023). URP: an integrated research platform for one-stop analysis of medical images. *Front. Radiol.* 3:1153784. doi: 10.3389/fradi.2023.1153784

Yazdan-Panah, A., Schmidt-Mengin, M., Ricigliano, V. A., Soulier, T., Stankoff, B., and Colliot, O. (2023). Automatic segmentation of the choroid plexuses: method and validation in controls and patients with multiple sclerosis. *Neuro Image: Clinical* 38:103368. doi: 10.1016/j.nicl.2023.103368

Yukun, Z., Liang, H., Rongfeng, Q., Qi, D., Shenyu, F., Xin, Z., et al. (2025). Impact of supine and upright positions on cerebral hydrodynamics in healthy subjects: a study using domestic multi-position helium-free MRI. *Chin. J. Magn. Reson. Imaging*, 1–8. Available online at: https://link.cnki.net/urlid/11.5902.R.20250609.2223.002

Zhao, L., Feng, X., Meyer, C. H., and Alsop, D. C. (2020). Choroid plexus segmentation using optimized 3D U-net. 2020 IEEE 17th international symposium on biomedical imaging (ISBI), IEEE, 381–384.

Glossary

Precentral_L - Left Precentral Gyrus

Precentral_R - Right Precentral Gyrus

Postcentral_L - Left Postcentral Gyrus

Postcentral_R - Right Postcentral Gyrus

Paracentral_L - Left Paracentral Lobule

Paracentral_R - Right Paracentral Lobule

Frontal_Sup_L - Left Superior Frontal Gyrus

Frontal_Sup_R - Right Superior Frontal Gyrus

Frontal_Mid_Rostral_L - Left Rostral part of the Middle Frontal Gyrus

Frontal_Mid_Rostral_R - Right Rostral part of the Middle Frontal Gyrus

Frontal_Mid_Caudal_L - Left Caudal part of the Middle Frontal Gyrus

Frontal_Mid_Caudal_R - Right Caudal part of the Middle Frontal Gyrus

Frontalpole_L - Left Frontal Pole

Frontalpole_R - Right Frontal Pole

Orbitofrontal_Lat_L - Left Lateral Orbitofrontal Cortex

Orbitofrontal_Lat_R - Right Lateral Orbitofrontal Cortex

Orbitofrontal_Med_L - Left Medial Orbitofrontal Cortex

Orbitofrontal_Med_R - Right Medial Orbitofrontal Cortex

Parsopercularis_L - Left Pars Opercularis

Parsopercularis_R - Right Pars Opercularis

Parsorbitalis_L - Left Pars Orbitalis

Parsorbitalis_R - Right Pars Orbitalis

Parstriangularis_L - Left Pars Triangularis

Parstriangularis_R - Right Pars Triangularis

Insula_L - Left Insula

Insula_R - Right Insula

Cingulum_Ant_L - Left Anterior Cingulum

Cingulum_Ant_R - Right Anterior Cingulum

Cingulum_Mid_L - Left Middle Cingulum

Cingulum_Mid_R - Right Middle Cingulum

Cingulum_Post_L - Left Posterior Cingulum

Cingulum_Post_R - Right Posterior Cingulum

Isthmuscingulate_L - Left Isthmus of Cingulate Cortex

Isthmuscingulate_R - Right Isthmus of Cingulate Cortex

Hippocampus_L - Left Hippocampus

Hippocampus_R - Right Hippocampus

Parahippocampal_L - Left Parahippocampal Gyrus

Parahippocampal_R - Right Parahippocampal Gyrus

Amygdala_L - Left Amygdala

Amygdala_R - Right Amygdala

Caudate_L - Left Caudate Nucleus

Caudate_R - Right Caudate Nucleus

Putamen_L - Left Putamen

Putamen_R - Right Putamen

Pallidum_L - Left Pallidum

Pallidum_R - Right Pallidum

Thalamus_L - Left Thalamus

Thalamus_R - Right Thalamus

Accumbens_Area_L - Left Nucleus Accumbens

Accumbens_Area_R - Right Nucleus Accumbens

VentralDC_L - Left Ventral Dorsal Cortex

VentralDC_R - Right Ventral Dorsal Cortex

Choroid_Plexus_L - Left Choroid Plexus

Choroid_Plexus_R - Right Choroid Plexus

Ventricle_Lat_L - Left Lateral Ventricle

Ventricle_Lat_R - Right Lateral Ventricle

Ventricle_Inf_Lat_L - Left Inferior Lateral Ventricle

Ventricle_Inf_Lat_R - Right Inferior Lateral Ventricle

Parietal_Sup_L - Left Superior Parietal Lobule

Parietal_Sup_R - Right Superior Parietal Lobule

Parietal_Inf_L - Left Inferior Parietal Lobule

Parietal_Inf_R - Right Inferior Parietal Lobule

Cuneus_L - Left Cuneus

Cuneus_R - Right Cuneus

Entorhinal_L - Left Entorhinal Cortex

Entorhinal_R - Right Entorhinal Cortex

Fusiform_L - Left Fusiform Gyrus

Fusiform_R - Right Fusiform Gyrus

Lingual_L - Left Lingual Gyrus

Lingual_R - Right Lingual Gyrus

Pericalcarine_L - Left Pericalcarine Cortex

Pericalcarine_R - Right Pericalcarine Cortex

Precuneus_L - Left Precuneus

Precuneus_R - Right Precuneus

Supramarginal_L - Left Supramarginal Gyrus

Supramarginal_R - Right Supramarginal Gyrus

Temporal_Sup_L - Left Superior Temporal Gyrus

Temporal_Sup_R - Right Superior Temporal Gyrus

Temporal_Mid_L - Left Middle Temporal Gyrus

Temporal_Mid_R - Right Middle Temporal Gyrus

Temporal_Inf_L - Left Inferior Temporal Gyrus

Temporal_Inf_R - Right Inferior Temporal Gyrus

Temporalpole_L - Left Temporal Pole

Temporalpole_R - Right Temporal Pole

Temporal_Sup_Banks_L - Left Superior Temporal Banks

Temporal_Sup_Banks_R - Right Superior Temporal Banks

Transversetemporal_L - Left Transverse Temporal Gyrus

Transversetemporal_R - Right Transverse Temporal Gyrus

Occipital_Lat_L - Left Lateral Occipital Cortex

Occipital_Lat_R - Right Lateral Occipital Cortex

Cerebral_WM_L - Left Cerebral White Matter

Cerebral_WM_R - Right Cerebral White Matter

Cerebellum_Cortex_L - Left Cerebellar Cortex

Cerebellum_Cortex_R - Right Cerebellar Cortex

Cerebellum_WM_L - Left Cerebellar White Matter

Cerebellum_WM_R - Right Cerebellar White Matter

Ventricle_3rd - Third Ventricle

Ventricle_4th - Fourth Ventricle

Pons - Pons

CSF - Cerebrospinal Fluid

Optic_Chiasm - Optic Chiasm

CC_Anterior - Anterior Corpus Callosum

CC_Mid_Anterior - Mid-Anterior Corpus Callosum

CC_Central - Central Corpus Callosum

CC_Mid_Posterior - Mid-Posterior Corpus Callosum

CC_Posterior - Posterior Corpus Callosum

Midbrain - Midbrain

Medulla - Medulla

SCP - Superior Cerebellar Peduncle